Noninvasive, Infrared Monitoring of Cerebral and Myocardial Oxygen Sufficiency and Circulatory Parameters

Abstract. *The relatively good transparency of biological materials in the near infrared region of the spectrum permits sufficient photon transmission through organs in situ for the monitoring of cellular events. Observations by infrared transillumination in the exposed heart and in the brain in cephalo without surgical intervention show that oxygen sufficiency for cytochrome a,a_3, function, changes in tissue blood volume, and the average hemoglobin-oxyhemoglobin equilibrium can be recorded effectively and in continuous fashion for research and clinical purposes. The copper atom associated with heme a_3 did not respond to anoxia and may be reduced under normoxic conditions, whereas the heme-a copper was at least partially reducible.*

When photons impinge on biological materials, their transmission depends on a combination of reflectance, scattering, and absorption effects. Reflectance is mainly a function of the angle of the light beam to the tissue surface, whereas the scattering and absorption are wavelength-dependent properties. Scattering decreases with increasing wavelengths, favoring thereby the transmission of infrared (IR) light. Absorption occurs at specific wavelengths, determined by the molecular properties of the materials in the light path. Thus variations occur in the effectiveness of transmission through animal tissues within the ultraviolet through the IR range. Above 1300 nm, water absorbs all photons over a pathlength of less than a few millimeters in normally hydrated tissues. In the visible part of the spectrum, below 700 nm, the intense absorption bands of hemoglobin (Hb) and increasing light scattering phenomena again prevent transmission over longer pathlengths. However, in the 700- to 1300-nm range of the near IR, a significant amount of radiation can be effectively transmitted through biological materials over longer distances.

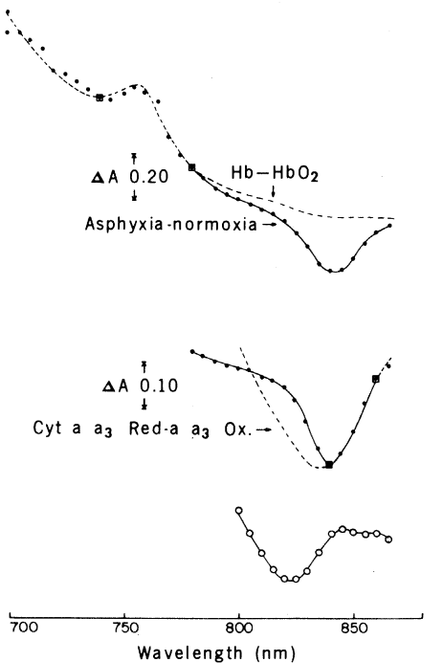

Fig. 1. (Top) Difference spectrum of a transilluminated cat's head between anoxia and normoxia. The data points (dots) conform to the difference spectrum of Hb minus HbO_2 (broken line) normalized at 740 and 780 nm (square points) except in the region above 780 nm. (middle). The 780- to 865-nm range after subtraction of the Hb-HbO_2 curve; drawn on a twice larger scale. The broken line shows the in vitro difference spectrum of purified reduced minus oxidized cytochrome a,a_3 normalized to the present data at 840 and 865 nm (*7*). (Bottom) The 800 to 865 nm region of purified cytochrome a,a_3 after subtraction of the present data from the purified enzyme difference spectrum.

Within this IR range cytochrome a,a_3 (cytochrome c oxidase), the terminal member of the respiratory chain has a weak absorption band. In his original description of the cytochromes, Keilin showed that the absence of oxygen resulted in the complete reduction of cytochrome a,a_3 (*1*). This conclusion was based on spectroscopic observations on the two heme moieties of the enzyme in the visible range. More recently it was shown that the two copper atoms of cytochrome a,a_3 follow this behavior (*2*). When oxidized, a weak absorption band exists in the 780- to 870-nm region of the near IR with a broad maximum from 820 to 840 nm. Upon reduction of the enzyme, this band disappears.

Cytochrome a,a_3 reacts directly with molecular oxygen. Transfer of four electrons from this enzyme to oxygen and concomitant or subsequent reaction with four hydrogen ions leads to the formation of two molecules of water. This final redox reaction of the respiratory chain accounts for more than 90 percent of all cellular oxygen utilization and, therefore, is of singular importance in cellular metabolism. Since more than 90 percent of cellular free energy is derived from the redox reactions of the chain, an insufficient supply of oxygen to cytochrome a,a_3 leads promptly to physiologic dysfunction and ultimately to cell death.

Because of the physiological importance of this enzyme and the favorable IR transmission characteristics in this range, it appeared useful to attempt to observe the oxygen dependent absorption peak in intact organs in vivo. In addition, disoxygenated Hb exhibits a weak absorption peak at 760 nm, whereas the oxygenated form (HbO_2) does not (*3*). Useful information on blood oxygenation in the tissue could therefore be expected if success in IR transmission could be achieved. Previous development of sensitive spectrophotometric techniques by Chance (*4*) provided means to measure in intact cells and excised tissues cytochrome absorption bands in the visible region (*5*). A modification of this technique appeared to hold promise for success.

The brain is most sensitively dependent on oxygen for normal function and is readily accessible with minimal interference of overlying tissues. Initial experiments on near IR monitoring of oxygen sufficiency for cellular function were, therefore, performed by transillumination of the cranium without surgery. Cats were anesthetized with pentobarbital (40 mg/kg), tracheotomized, intubated, and provided with femoral arterial and venous cannulas. Hair was removed over two areas (approxmately 2 cm^2 each) at both temples by a depilatory agent. The head was immobilized in a stereotaxic holder and light-conducting optic fiber bundles were applied with firm pressure against the skin at both

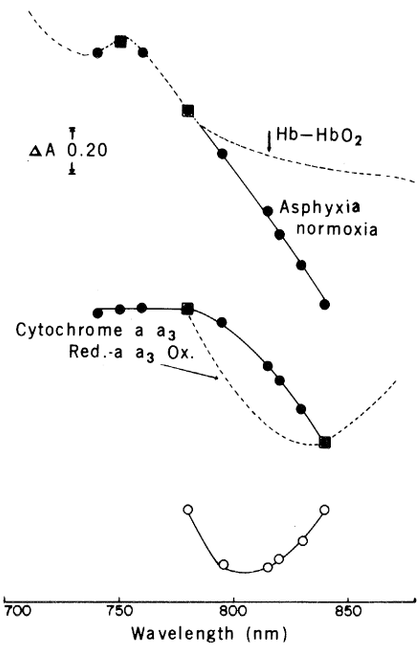

Fig. 2. Anoxic-normoxic difference spectrum of a transilluminated dog heart in situ and its analysis in various components. The figure was constructed as described in the text and in the legend to Fig. 1.

temples. One, a Y-shaped bundle, transmitted the appropriate wavelengths of near IR radiation from two monochromators to one temple, the other conducted the light emerging from the opposite side of the head to an IR sensitive photomultiplier tube (Hamamatsu R928) for detection and measurement. Two 6.6-nm spectral bands were presented alternately at a repetition rate of 60 hertz. Appropriate electronic circuits amplified and demodulated the separate signals, converted them to d-c and subtracted them by means of a differential amplifier for a difference readout (*6*). One wavelength band served as reference for the other (sample) band. For the reference wavelength the isobestic point of Hb-HbO_2 at 815 nm was selected. A negative feedback circuit on the high voltage source supplying the photomultiplier stabilized the reference signal against absorption changes in the tissue at that wavelength. In the subsequent interval, when the sample wavelength was presented, this high voltage was maintained. Thus, the differential measurements were corrected for variations in cerebral blood volume. As an additional benefit, the voltage changes in the photomultiplier supply became indicative of the changes in blood volume in the optical path and were, therefore, also recorded (*6*).

The sample wavelength was varied in steps, first in the normoxic state, then in anoxia after asphyxiation (Fig. 1, top curve). These results are ascribed to cerebral reactions since contributions from extracerebral tissues were found to be negligible in separate experiments. At lower wavelengths (740 to 780 nm) the data points conform satisfactorily to the normalized difference spectrum of Hb-HbO_2. At higher wavelengths (780 to 865 nm) the significant trough in the cytochrome a,a_3 absorption region has a minimum at approximately 840 nm (ranging from 834 to 851 nm in separate experiments) (Fig. 1, middle curve) (*7*). The greater sharpness of the in vivo data is interpreted as showing a missing component in the cytochrome a,a_3 band. Subtraction of the in vivo from the in vitro curve, shown in the bottom curve of Fig. 1, reveals the maximal difference at 822 nm (810 to 822 nm in separate experiments). Administration of a gas mixture of 15 percent carbon dioxide and 85 percent oxygen to artificially ventilated animals resulted in an inverted spectrum of approximately the same shape though somewhat broader in the 800- to 860-nm range than the one shown in Fig. 1. The absorption maximum was found to occur at 820 nm (813- to 828-nm range in separate experiments). This is interpreted as showing that the "missing component" does respond to increased O_2 availability. Some increased optical density at 840 nm, resulting in the greater breadth of the absorption band in hyperoxia, indicated an oxidation of the 840 nm component as well.

Recent results of Chance and Leigh (*8*) indicate that, in the oxidized state, the copper more closely associated with the heme a_3, the so-called high potential copper (Cu_H), contributes mainly to the lower wavelength part of the near IR band. Oxidized low potential copper (Cu_L) associated with heme a, predominates at the higher wavelengths. Both lose most of their absorbance when reduced. From this consideration and from confirming experiments in vivo on cyanide inhibition of cytochrome a,a_3, it is concluded that the relatively narrow 840-nm trough results from the reduction of Cu_L. Apparently even in normoxia the steady-state redox level of the Cu_H population is already practically completely reduced. However, a significant fraction of the Cu_L is oxidized, which agrees with the partial oxidation (15 percent) of heme a observed in the exposed brain by reflection spectrophotometry (*9*). The quantitative assessment of the degrees of oxidation of the two copper atoms in normoxia must await experiments on complete oxidation with hyperbaric oxygen or other oxidizing agents.

Similar experiments were also performed on the exposed dog's heart in situ. The entry optic fiber bundle was placed against the pericardium with sufficient pressure to contact the right side of the heart slightly above the apex. On the opposite side a massive (2.5 cm in diameter) bundle collected the transmitted IR light. It was focused on the end window of a cooled photomultiplier by means of accessory optics (DIL, Inc.) (*10*). Because of the large volume of blood in the chambers, the attenuation of IR light was significantly greater than in the experiments on the cat's head. Measurement of the photomultiplier current was precluded and a photon counting technique (Ortec, Inc.) was used instead. Even so, through a combination of decreasing photomultiplier sensitivity and light intensity, the signal above 840 nm was too weak to allow the collection of meaningful data.

Under steady illumination ten counting periods of 10 seconds each were first recorded at a number of wavelength settings under normoxic, artificial respiration. After anoxic death by asphyxia,

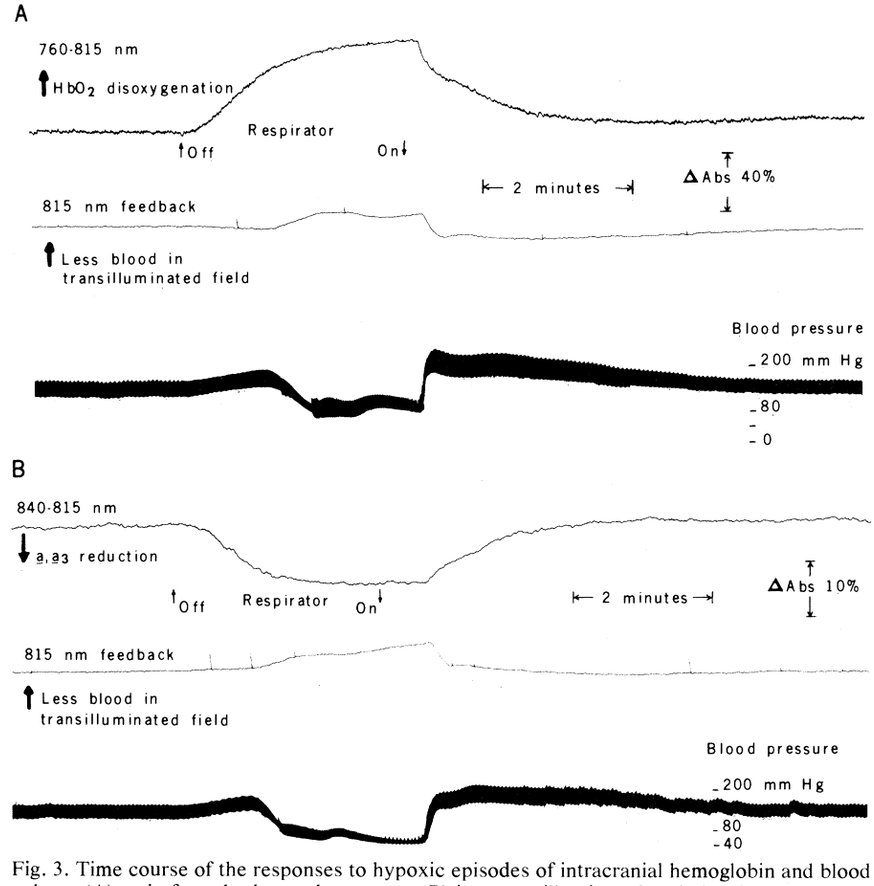

Fig. 3. Time course of the responses to hypoxic episodes of intracranial hemoglobin and blood volume (A) and of cerebral cytochrome a,a_3 (B) in a transilluminated cat's head.

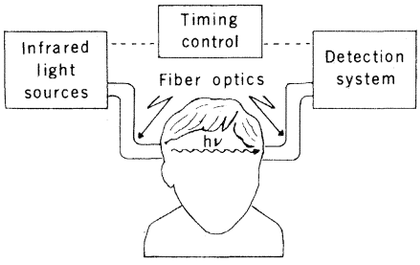

Fig. 4. Infrared monitoring of cerebral circulation and oxygen sufficiency.

counting was repeated. The resulting data were converted to the change in absorbancy (ΔA) and are shown in Fig. 2. The spectrum above 800 nm shows a larger decrease in the light absorption characteristics than in the Hb-HbO_2 spectrum. The shift toward a more narrow band at higher wavelengths than for cytochrome a,a_3 is revealed. When the in vitro cytochrome a,a_3 difference spectrum is subtracted, the missing lower band is found to be centered around 810 nm approximately (810 to 815 nm in separate experiments).

Kinetic measurements were made on cerebral hemoglobin and cytochrome a,a_3 during temporary apnea produced by interruption of the artificial respiration for 3 minutes after the animal was paralyzed. In the top trace of Fig. 3A the signal at 760 minus 815 nm indicates the change of hemoglobin from a partially arterial to a more venous condition, $HbO_2 \rightarrow Hb$. The middle trace represents the negative voltage supplying the photomultiplier after feedback stabilization for constant reference signal (815 nm). The rise in the trace indicates a decreasing absorbancy at this Hb-HbO_2 isobestic point during the fall in blood pressure (lower trace). Apparently a measurable change in blood volume in the brain occurs when the circulation starts to fail (Fig. 3B).

Experimentation has been extended to the human brain. Because of the much greater pathlength (13.3 cm) as compared to the cat's head (approximately 5 cm, average) and consequent loss of IR intensity, photon counting was required. The optic fiber bundles were placed somewhat above and frontal to the temples in order to avoid the masseter muscles (Fig. 4). Blood volume was monitored in this fashion at 815 nm, the Hb-HbO_2 isobestic point. The counts were significantly above background (darkness) over 10-second counting periods (t-test, $P \ll .001$). Voluntary hyperventilation, which decreases cerebral circulation by hypocapnia, was used as a functional test.

A significant decrease in absorbancy, reflected in increased net counts (total counts minus background) was observed in sequential counting periods (Fig. 5). This decrease was correlated with statements by the subject who reported increasing degrees of dizziness starting in the third counting period. After the fifth period the subject felt too dizzy to continue and hyperventilation was terminated. Thus, partial cerebral ischemia was monitored.

The results indicate that a "window" for effective transmission of near IR light exists in biological materials and that cerebral Hb-HbO_2 steady states, the blood volume, the redox state of cytochrome a,a_3, and thereby oxygen sufficiency can be monitored noninvasively. In addition, ongoing animal experiments show that cerebral blood flow rates can be measured quantitatively by means of close arterial injection of IR absorbing dyes or by a single-breath carbon monoxide technique (*11*). Myocardial measurements in situ without surgical intervention have as yet not been accomplished, although photon counts, statistically significant above background, have been recorded through the dog's chest over 20-second counting periods (t-test, $P < .001$). Further development of this technique for the myocardium must emphasize resolution within a single beat. This approach is awaiting improved instrumentation, especially in the form of higher intensity light sources.

The ability to monitor, continuously and noninvasively, oxygen sufficiency and circulatory parameters holds promise for a number of applications. The limiting factor at this moment appears to be the means of delivering sufficient light energy at selected wavelengths. The maximal intensity used in these studies was 48 $\mu w\ cm^{-2}$ in a 6.6-nm wide band. This compares with the intensity of sunlight of approximately 300 μw in a 6.6-nm band in the same region, or more than 10 $mw\ cm^{-2}$ in the entire near IR window, and the 500 $mw\ cm^{-2}$ level now allowed by national laser safety standards. Our studies are aimed at application of this technique to the monitoring of adequacy of intracellular oxygenation in clinical ischemia and hypoxemia.

The observation of a highly reduced steady state of the Cu_H atom of cytochrome a,a_3 is in disagreement with the highly oxidized state of the heme-a_3 iron of this enzyme in isolated mitochondria in vitro (*12*). High reduction levels of the cytochromes, including cytochrome a,a_3, have, however, been observed in a number of intact tissues (*13*), including the heart (*14*) and the normally perfused,

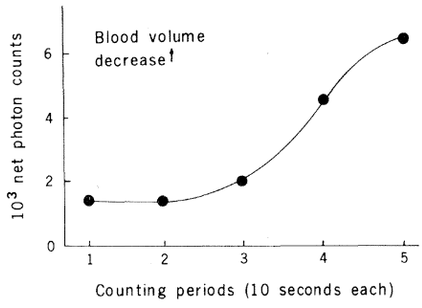

Fig. 5. Restriction of cerebral blood volume during voluntary hyperventilation. The subject was a healthy, 47-year-old, male, white volunteer with a larger than average head (13.3 cm diameter at the temples). The area of the light entry fiber bundle was 0.567 cm^2. The 10-second counting periods were interspersed with 1-second intervals for readout. Hyperventilation was started shortly before the beginning of the first counting period.

exposed cerebral cortex (*6, 9, 15*). From the above data it appears that in vivo a partial block between Cu_H and oxygen exists and accounts for the high reduction levels, which are lost during the preparation of mitochondria for experimentation in vitro.

FRANS F. JÖBSIS

Department of Physiology, Duke University, Durham, North Carolina 27710

References and Notes

1. D. Keilin, *Proc. Roy. Soc. London Ser. B*, **98**, 312 (1925).
2. D. E. Griffiths and D. C. Wharton, *J. Biol. Chem.* **236**, 1857 (1961); B. Chance, in *The Biochemistry of Copper*, J. Peisach, P. Aisen, W. E. Blumberg, Eds. (Academic Press, New York, 1966), pp. 293–300.
3. O. W. Van Assendelft, *Spectrophotometry of Haemoglobin Derivatives* (Thomas, Springfield, Ill., 1970).
4. B. Chance, *Science* **120**, 3124 (1954); *Rev. Sci. Instr.* **22**, 634 (1951).
5. A. Weber and B. Chance, *J Physiol. London* **169**, 263 (1963). F. F. Jöbsis, *J. Gen. Physiol.* **46**, 905 (1963); ———, in *Handbook of Physiology: Respiration 1* (American Physiological Society, Washington, D.C., 1964), chap. 2.
6. F. F. Jöbsis, J. H. Keizer, J. C. LaManna, M. Rosenthal, *J. Appl. Physiol.* **43**, 858 (1977).
7. D. C. Wharton and A. Tzagoloff, *J. Biol. Chem.* **239**, 2036 (1964).
8. B. Chance and J. S. Leigh, *Proc. Natl. Acad. Sci. U.S.A.*, in press.
9. F. G. Hempel, F. F. Jöbsis, J. C. LaManna, M. Rosenthal, H. A. Saltzman, *J. Appl. Physiol.* **43**, 873 (1977).
10. The success of this research was fostered by the advice and technical support of the Durham Instrumentation Laboratory, Inc. (DIL), in the design and construction of the light fiber bundles and accessory optics.
11. J. M. Colacino, B. Grubb, F. F. Jöbsis, *Circ. Res.*, in press.
12. B. Chance and G. R. Williams, *J. Biol. Chem.* **217**, 383 (1955).
13. S. J. Hersey and F. F. Jöbsis, *Biochem. Biophys. Res. Commun.* **36**, 243 (1969); S. J. Hersey, W. L. High, F. F. Jöbsis, in *Gastric Secretion* (Academic Press, New York, 1972), p. 239; S. J. Hersey, *Biochim. Biophys. Acta.* **344**, 157 (1974); E. Mills and F. F. Jöbsis, *J. Neurophysiol.* **35**, 405 (1972); L. J. Mandel, D. F. Moffett, F. F. Jöbsis, *Biochim. Biophys. Acta.* **408**, 123 (1975); D. F. Moffett and F. F. Jöbsis, *Brain Res.* **117**, 239 (1976); F. F. Jöbsis and J. C. LaManna, in *The Extrapulmonary Manifestations of Respiratory Diseases*, E. D. Robin, Ed. (Dekker, New York, in press).
14. J. Ramirez, *J. Physiol.* **147**, 14 (1959); I. E. Hassinen and K. Hiltunen, *Biochim. Biophys. Acta*

408, 319 (1975); T. R. Snow, A. S. Wechsler, F. F. Jöbsis, L. M. Kleinman, J. C. LaManna, *Proc. Fed. Assoc. Soc. Exp. Biol.* **36**, 518 (1977).
15. F. F. Jöbsis, M. Rosenthal, J. C. LaManna, E. Lothman, G. Cordingley, G. Somjen, in *Brain Work, Alfred Benzon Symposium VIII*, D. H. Ingvar and E. Lassen, Eds. (Munksgaard. Copenhagen, 1975); G. Austin, G. Haugen, J. C. LaManna, in *Oxygen and Physiological Function*, F. F. Jöbsis, Ed. (Professional Information Library, Dallas, Tex., 1977).
16. I thank J. H. Keizer, R. F. Overaker, M. M. Grafton, B. J. Comfort, J. A. Cannon, and A. Scagnelli for assistance in various aspects of the work; Drs. J. M. Colacino, F. G. Hempel, J. C. LaManna, L. J. Mandel, M. Rosenthal, H. A. Saltzman, T. R. Snow, and A. L. Sylvia for advice, support, and criticism; and Dr. B. Chance for supplying various unpublished data and for helpful discussions. Partially supported by NIH grants 1RO1 HL 17391, NS 06233, and NS 13319.

4 May 1977; revised 24 August 1977

Neuronal Architecture of On and Off Pathways to Ganglion Cells in Carp Retina

Abstract. *Bipolar, amacrine, and ganglion cells of carp retina, stained intracellularly with Procion yellow, can be divided into types a and b, according to the destination of terminals and dendritic trees in the inner plexiform layer (sublamina a and b, respectively). Type a cells showed hyperpolarizing, or off, responses and type b cells depolarizing, or on, responses. Carp thus resembles cat in the basic organization of on and off pathways in the retina.*

The inner plexiform layer (IPL) of cat retina can be divided into two sublaminae, one of which contains the terminals of "flat" cone bipolar cells (sublamina "a") and the other of which contains the terminals of "invaginating" cone bipolars (sublamina "b") (*1*). Moreover, the majority of retinal ganglion cells can be divided into types "a" and "b", according to the sublamina in which their dendritic trees are confined (*1*). It was proposed that sublamina a, nearest the amacrine cell bodies, contains the synaptic connections for off-center ganglion cells and sublamina b, nearest the ganglion cells, the connections for on-center ganglion cells (*1*). This hypothesis has been confirmed in the retina of the cat by iontophoresis of fluorescent dyes into ganglion cells, after intracellular recording of their responses (*2*).

We now report the results of a similar analysis applied to the retina of the carp, in which two advantages are obtained for examination of this hypothesis: (i) the distinctive stratification of the IPL (*3*) is much easier to appreciate in carp retina than in most mammalian retinas and is especially prominent under fluorescent light, and (ii) it is relatively easy to record from and to stain cyprinid bipolar and amacrine cells (*4*). Despite the very distant phylogenetic relationship of carp and cat, we find that all carp neurons contributing processes to the IPL (bipolar, amacrine, and ganglion cells) also follow the rule that cells branching in sublamina a [Cajal's strata (S) 1, 2, and 3 in carp] give hyperpolarizing (off) responses, and those branching in sublamina b (S4 and S5 in carp), give depolarizing (on) responses (*5*).

Retinas of light-adapted *Cyprinus carpio* were isolated in dim light with the receptor side up and transferred to a superfusion chamber, where they could be maintained in good condition for about 2 hours (*6*). Retinas of fish that were dark-adapted for more than 40 minutes were prepared in dim red light. Microelectrodes containing a 4 percent solution of Procion yellow MX-4R had resistances of 200 to 300 megohms; neurons were penetrated by electrical oscillation of the preamplifier applied to the electrode tip through the capacitance compensation feedback circuit. Each cell was identified by its response to 400-msec flashes of white or monochromatic lights of equal quanta, projected onto the retina as small spots (60 to 240 μm) or annuli (inside diameter, 0.5 mm; outside diameter, 3.5 mm) in a dual beam system in the presence of a background light (*7*). Dark-adpated retinas were studied without background light, with stimuli attenuated by 4 log units more than in photopic studies. Dye was passed through the electrode tip with 2 to 3 na of direct current for 200 to 600 seconds. Retinas were fixed in buffered aldehydes (*p*H 7.2), embedded in Spurr mixture E, sectioned at 15 μm, and examined with dark-field flu-

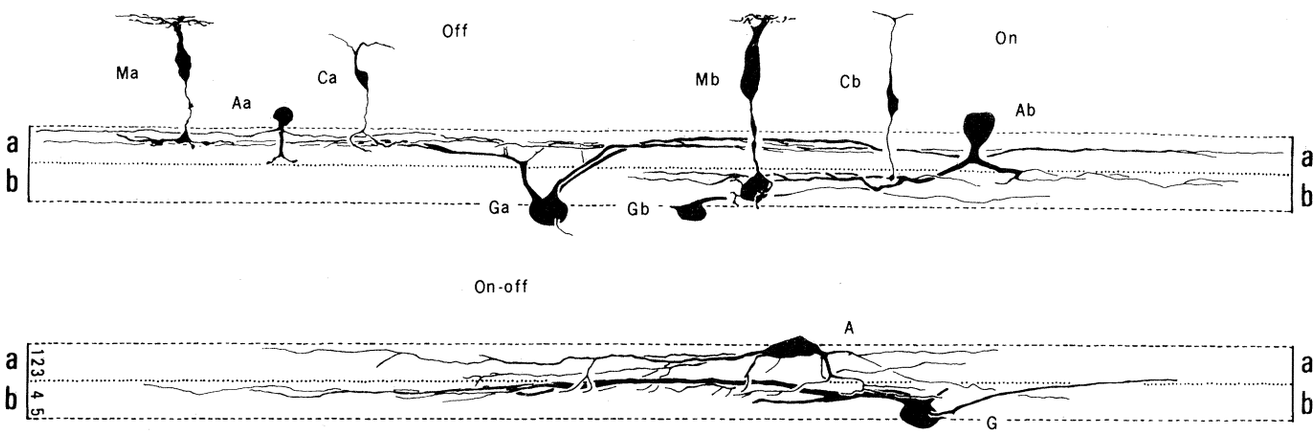

Fig. 1. Drawings of bipolar, amacrine, and ganglion cells in the retina of the carp, stained with Procion yellow after intracellular recording of their responses (Fig. 2). All cells send synaptic processes into the inner plexiform layer (IPL), which is divided into two sublaminae, a and b, about equally thick. Sublamina a is composed of strata 1, 2, and 3, while sublamina b includes only strata 4 and 5. Synaptic processes of type a cells are confined to sublamina a, and those of type b cells to sublamina b. The former are all hyperpolarizing (off) in their responses, while the latter are all depolarizing (on) (see Fig. 2). Bipolar cells are of two main varieties: large "M" bipolars and small "C" bipolars. Ma bipolars end in strata 1 and 2, and Mb bipolars in strata 4 and 5 with large globular terminals. Many varieties of amacrine cells were stained, three of which are shown here. "Ab" is the most commonly found sustained amacrine, and "A" is the typical on-off amacrine, the former confined to stratum 4 and the latter broadly stratified in S1 through S4. "Aa" is a bistratified amacrine, but is confined to sublamina a and is hyperpolarizing (Fig. 2). Though unusual in appearance, this cell appears to be almost completely stained. "Ga" is an example of Cajal's "giant" ganglion cell, branching at the border of S1 and S2. "Gb" represents one of the few type b (on) ganglion cells of which any dendrites were stained. "G" is typical of the large on-off ganglion cells. Dendritic branches enter both sublaminae, strata 3 and 4. Scale: thickness of the IPL is 40 μm.